

# Clinical correlation of imaging findings in congenital cranial dysinnervation disorders involving abducens nerve

Chanchal Gupta, Pradeep Sharma, Rohit Saxena, Ajay Garg<sup>1</sup>, Sanjay Sharma<sup>2</sup>

**Purpose:** High-resolution magnetic resonance imaging (MRI) of intracranial parts of sixth nerve and seventh nerve and the extraocular muscles (EOMs) in orbit to correlate the clinical characteristics in patients with two special forms of strabismus in congenital cranial dysinnervation disorders which are Duane's retraction syndrome (DRS) and Mobius syndrome. **Materials and Methods:** Morphological analysis by 3T MRI of orbit (using surface coils) and brain (using 32 channel head coil) was performed on 6 patients with clinical DRS (1 bilateral), 2 cases with Mobius syndrome, and 1 case with congenital sixth nerve palsy. These were compared with findings in five controls. **Results:** We observed absence/hypoplasia of sixth nerve in five out of seven eyes with DRS (71.42%), anomalous course in one eye, sixth and seventh nerve absence/hypoplasia in affected eyes with Mobius syndrome and bilateral absence/hypoplasia of the sixth nerve in congenital sixth nerve palsy. For EOMs we calculated maximum diameter, area, and circumference of muscles using Osirix software, and noticed significant hypoplasia of lateral rectus in comparison to controls ( $P < 0.001$ ). **Conclusions:** MRI gives useful information regarding confirmation of clinical diagnosis and its neurological anomalies in complex cases and helps to plan tailor made surgical management.

**Key words:** Congenital cranial dysinnervation disorder, Duane's retraction syndrome, magnetic resonance imaging brain, magnetic resonance imaging orbit

Congenital cranial dysinnervation disorders (CCDDs) are reported to be secondary to some neurologic pathology of congenital origin and have a wide spectrum of phenotypic presentation which is due to either primary or secondary dysinnervation. These were thought of as primary myopathies, but now with available literature, these are proved to be primary neurogenic disorders, in which one or more nerves are affected, and abnormal synkinesis develops leading to various presentations of these disorders. A term CCDD<sup>[1,2]</sup> was given to these disorders by Gutowski *et al.* Duane's retraction syndrome (DRS) and Mobius syndrome are common forms, in which the sixth nerve is involved, and neuroimaging in these disorders can help us in understanding the pathophysiology and clinical picture associated. Our study aims to evaluate changes in cranial nerves supplying the orbit and extraocular muscles (EOMs) in DRS and Mobius syndrome and use it to explain the clinical presentation of the cases.

## Materials and Methods

This was a pilot study where patients were recruited from the squint clinic of a tertiary eye care center with a clinical diagnosis of DRS, Mobius syndrome, and congenital sixth nerve palsy. Written informed consent was obtained from all patients/guardians, and the study protocol was approved by the Institutional Ethics Committee. Five controls (concomitant

squint) were chosen and explained about the procedure, and a similar consent was taken. All subjects and controls underwent complete eye examinations, in which corrected vision, anterior and posterior segment, ductions and versions were evaluated.

Subjects underwent complete ophthalmologic examination which included measurement of binocular misalignment by prism in all nine gazes, documentation, and measurement of head posture if any, the presence of binocularity and measurement of stereoacuity if present as well as documentation of associated clinical features related to our diagnosis as crocodile tears. Age criteria were set as over 8 years so that the patient could cooperate for magnetic resonance imaging (MRI), without anesthesia or sedation.

The MRI examination was done on 3T scanner (Achieva QX, Philips; Netherlands). The patient was asked to lie supine on scanner table. Medium size surface coil was used for orbital imaging which was fixed on eye to be imaged with adhesive bands. The other eye was patched to avoid diplopia or alternate fixation in a narrow scanner gantry. Head was turned 23° toward the opposite side of eye to be imaged<sup>[3]</sup> so that eye came in a position, in which visual axis and orbital axis were same (quasicoronal view). A point target for fixation (bright adhesive tapes with dark spot in center) was provided to the patient, which the patient affixed

### Access this article online

#### Website:

www.ijo.in

#### DOI:

10.4103/ijo.IJO\_1013\_15

### Quick Response Code:



Department of Ophthalmology, Dr. Rajendra Prasad Centre for Ophthalmic Sciences, <sup>1</sup>Department of Neuroradiology, All India Institute of Medical Sciences, <sup>2</sup>Department of Radiodiagnosis, Dr. Rajendra Prasad Centre for Ophthalmic Sciences, New Delhi, India

**Correspondence to:** Prof. Pradeep Sharma, Room No. 484, Dr. Rajendra Prasad Centre for Ophthalmic Sciences, All India Institute of Medical Sciences, New Delhi, India. E-mail: drpsharma57@yahoo.com

**Manuscript received:** 28.12.15; **Revision accepted:** 30.01.17

This is an open access article distributed under the terms of the Creative Commons Attribution-NonCommercial-ShareAlike 3.0 License, which allows others to remix, tweak, and build upon the work non-commercially, as long as the author is credited and the new creations are licensed under the identical terms.

**For reprints contact:** reprints@medknow.com

**Cite this article as:** Gupta C, Sharma P, Saxena R, Garg A, Sharma S. Clinical correlation of imaging findings in congenital cranial dysinnervation disorders involving abducens nerve. Indian J Ophthalmol 2017;65:155-9.

himself inside of coil centered on straight ahead gaze to avoid motion artifacts. Gantry fan was kept off to decrease patient discomfort by tear evaporation while the patient was fixing. The patient was instructed from outside to fixate the target and avoid blinking during scan time. First localizer sequence was taken, followed by axial scan of the head, on which planning for quasicoronal and quasisagittal sections of orbit was done. The area was chosen as anteriorly from muscle insertion to posteriorly up to orbital apex. For quasicoronal image plane was kept perpendicular to the optic nerve and for sagittal parallel to it. Two-millimeter thick sections with total of 22 sections were obtained for each quasicoronal and sagittal section.

For evaluation of cranial nerve, 32-channel phased-array head coil was used, again head was fixed, and patients were told to keep eyes closed as we did not need fixation for these scans. First localizer scan was taken, on which planning for further sequences was done. Brain stem imaging was done with thin sections of 1 mm. IAC and three-dimensional (3D)

T1 sequences were run on which for interpretation we could do multiplanar reconstruction. The above imaging protocol was standardized and pretested for orbital imaging, and the imaging parameters are given below in Table 1.

For interpretation 3D drive sequence, we could see cisternal segment of abducens nerve, where it could be best seen in contrast to background hyperintense cerebrospinal fluid (CSF) surrounding hypointense nerves on T2-weighted images. Sixth nerve was traced above the level of seventh and eighth nerve and below the level of the fifth nerve, exiting from pons traversing through CSF near vertically, finally to enter into Meckel's cave. Examination of contiguous thin image planes avoided the possibility of missing small structure between sections and permitted confirmation of structures by their presence in contiguous planes.

For orbital imaging, we acquired 2 mm thick slices with no interslice gap, starting from muscle insertions on globe to orbital apex. We selected the fifth slice behind the globe, i.e., 10 mm

**Table 1: Magnetic resonance imaging protocol for imaging**

Name of scan	Brain imaging			Orbit imaging		
	T2W TRA brain clear	T2W, 3D drive sensitivity encoding	T1W, 3D TFE sensitivity encoding	T2W TSE, FS clear	T1W SE, COR-HR clear	T1W SE, SAG SE clear
Duration (month)	1:48	3:38	7:29	2:24	6:30	6:38
Scan technique	TSE	TSE	T1-TFE	TSE	SE	SE
Images	27	120	160	20	15	22
TR/TE (ms)	3000/80	2000/200	8.3/3.8	3000/80	589.7/12	589.7/12
Flip angle (°)	90	90	8	90	90	90
FOV (mm)	230	150	240	220	60	60
ACQ voxel size (mm)	0.58/0.72/4.0	0.59/0.99/1.0	1/1/1	1.10/1.47/2.0	0.6/0.54/2.0	0.6/0.54/2.0
Slice thickness/interslice thickness (mm)	4/1	1/0.5	1/0	2/0	0.6/0.54/2.0	2/0

T2W: T2-weighted, T1W: T1-weighted, TFE: Turbo fast echo, TSE: Turbo spin echo, SE: Spin echo, TR/TE: Repetition time/echo time, FOV: Field of view, ACQ: Acquisition, 3D: Three-dimensional, SAG: Sagittal, COR: Coronal, HR: High resolution, FS: Fat suppression, TRA: Transverse

**Table 2: Clinical examination of all patients**

Diagnosis	BCVA		Clinical features					Other features
	Right	Left	Horizontal deviation (PP)	Head turn	Up shoot	Down shoot	Bino cularity	
Case 1 bilateral DRS	1.0	1.0	2 PDXT	N	N	N	Y	-
Case 2 left eye DRS	1.0	1.0	20 PDET	Y	Y	Y	Y	
Case 3 right eye DRS	1.0	1.0	30 PDXT	Y	Y	Y	Y	Crocodile tears
Case 4 right eye DRS	1.0	1.0	25 PDXT	Y	Y	Y	Y	
Case 5 left eye DRS	1.0	1.0	20 PDXT	Y	Y	N	Y	
Case 6 left eye DRS	1.0	1.0	8 PDET	Y	N	N	Y	Crocodile tears, history of seizures
Case 7 Mobius with left seventh nerve palsy	1.0	<0.1	45-50 PDET	N	N	N	N	Deviation of angle of mouth, absent nasolabial fold
Case 8 Mobius with the left seventh nerve palsy	1.0	1.0	8-10 PDET	N	N	N	N	Deviation of angle of mouth to right, absent nasolabial fold
Case 9 bilateral congenital sixth nerve palsy	0.1	0.5	50 PDET	N	N	N	N	

PP: Primary position, PD: Prism diopter, XT: Exotropia, N: Absent, Y: Present, ET: Esotropia, DRS: Duane's retraction syndrome, BCVA: Best-corrected visual acuity

**Table 3: Measurements of lateral rectus in terms of maximum diameter, area, and circumference in cases**

	Affected eyes			Unaffected eyes		
	LRD (cm)	LRA (cm <sup>2</sup> )	LRC (cm)	LRD (cm)	LRA (cm <sup>2</sup> )	LRC (cm)
Case 1						
Right eye	0.89	0.25	2.10			
Left eye	0.77	0.26	1.98			
Case 2	0.90	0.28	2.18	1.13	0.37	2.63
Case 3	1.06	0.29	2.55	0.93	0.33	2.40
Case 4	0.93	0.33	2.40	1.07	0.29	2.54
Case 5	0.89	0.29	2.22	1.02	0.35	2.47
Case 6	0.66	0.07	1.41	1.04	0.33	2.48
Case 7	0.98	0.30	2.39	0.97	0.29	2.45
Case 8	0.69	0.14	1.70	0.98	0.26	2.30
Case 9						
Right eye	0.74	0.28	2.03			
Left eye	0.76	0.20	2.12			

LRD: Lateral rectus diameter, LRA: Lateral rectus area, LRC: Lateral rectus circumference

**Table 4: Measurements of lateral rectus in terms of maximum diameter, area, and circumference in controls**

	LRD (cm)	LRA (cm <sup>2</sup> )	LRC (cm)
Control 1			
Right eye	1.17	0.38	2.69
Left eye	1.21	0.37	2.85
Control 2			
Right eye	0.92	0.35	2.32
Left eye	1.21	0.36	2.44
Control 3			
Right eye	1.08	0.36	2.71
Left eye	1.12	0.31	2.54
Control 4			
Right eye	1.03	0.31	2.39
Left eye	1.09	0.28	2.55
Control 5			
Right eye	0.91	0.32	2.34
Left eye	1.00	0.38	2.47

LRD: Lateral rectus diameter, LRA: Lateral rectus area, LRC: Lateral rectus circumference

behind the globe where muscle belly lies, and maximum changes are described in posterior orbit. Using Osirix software (Macintosh platform) maximum diameter, area and circumference of muscles were measured by single person who was unaware of subject being a case or control. 3D T1-weighted images for whole brain were reconstructed in different planes to look for associated brain malformations.

For analysis, we compared muscle size in terms of maximum diameter, area, and circumference in affected and unaffected eyes of cases in comparison to controls, we analyzed our findings for ordinal data (values in muscle measurements) using ANOVA, and further intergroup comparison was done by *post hoc* tests. We labeled muscle to be hypoplastic when at least two variables were statistically significant.

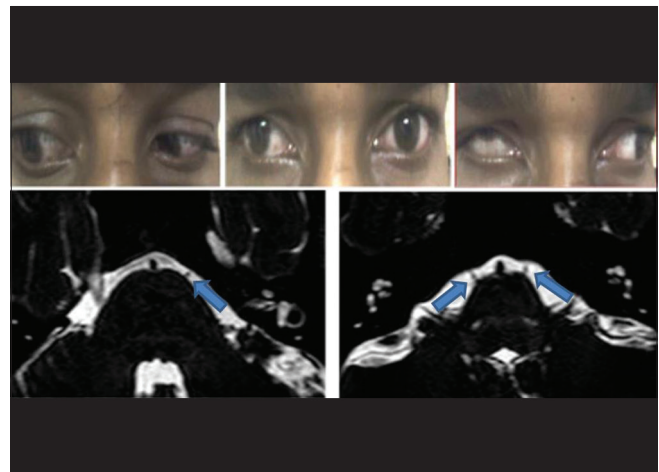


**Figure 1:** Clinical picture of case 4 showing exodeviation in primary gaze and severe retraction of globe and upshoot in attempted levoversion. MRI of same patient showing absence of right sided 6<sup>th</sup> nerve (left with arrow) compared with presence of bilateral 6<sup>th</sup> nerves (arrows) in control subject

## Results

A total of six patients with DRS Type 1 (one bilateral), two patients with Mobius syndrome and one patient with congenital bilateral sixth nerve palsy, and 5 age-matched controls participated in the study. Clinical examination of the patients is given in Table 2. We found absence or hypoplasia of sixth nerve in 5 out of 7 eyes with DRS (71.42%) as shown in Fig. 1 showing clinical picture of Case 4 along with MRI image of same patient, anomalous course in one eye as shown in Fig. 2 showing clinical picture of Case 2 with MRI image; sixth and seventh nerve absence/hypoplasia in two patients with Mobius syndrome. Bilateral absence/hypoplasia of sixth nerve was present in a patient with congenital sixth nerve palsy. For EOMs, we calculated maximum diameter, area, and circumference of muscles using Osirix software for both cases and controls; same is given in Tables 3 and 4. The mean

value for all measurements is given in Table 5 with respective *P* values. There was significant hypoplasia of lateral rectus in affected eyes, and this was consistent in segregated group of DRS patients also whereas clinically unaffected eyes, as well as other EOMs, had no significant difference from controls. Splitting of lateral rectus was seen in the right eye of case 9 (B/L sixth nerve palsy) as in Fig. 3. We found dolichoectasia of basilar artery in a patient with esotropic DRS (Case 6) and ipsilateral pontine dysplasia in one patient of Mobius syndrome (Case 8).

**Discussion**

Gutowski *et al.*<sup>[11]</sup> coined a term “Congenital cranial dysinnervation disorders” for congenital disorders resulting from aberrant innervation of the ocular and facial musculature. Use of MRI now gives us the opportunity for evaluating the anatomy of EOMs and surrounding connective tissue in the orbits of living subject, and the cranial nerves can be imaged where they exit the brain stem. Most of the previous studies have used 1.5T MRI for this purpose, but we used 3T MRI as it has better resolution and more signal to noise ratio.<sup>[4,5]</sup>

Our interpretations regarding hypoplasia of sixth nerve in these disorders were comparable to the previous literature.<sup>[6-9]</sup>

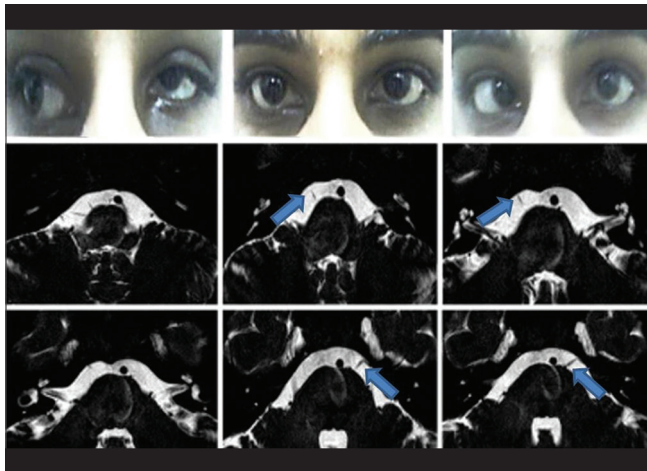


**Figure 2:** Clinical picture of Case 2 (left esotropic Duane’s retraction syndrome) showing left esodeviation in primary gaze and limitation of abduction in attempted levoversion and globe retraction on attempted dextroversion followed by sequential section magnetic resonance imaging at pons showing right-sided sixth nerve (arrow) in cisternal segment and left sixth nerve (arrow) exiting at higher level from pons and taking horizontal course in comparison to the right side and entering into Meckel’s cave

Cause for different presentations in different syndrome is the amount and time of development of coinnervation. We found statistically significant lateral rectus hypoplasia in affected eyes of cases in comparison of controls though previous studies<sup>[7,10]</sup> show normal bulk of lateral rectus in DRS patients as compared to sixth nerve palsy and explained this by coinnervation. This variation from the previous studies could be due to variable spectrum of presentation in DRS. We can say coinnervation can preserve lateral rectus muscle mass in few patients but not in all. Other possibility is fibrosis of muscle to some extent has already occurred before coinnervation develops as EOMs innervated by the impaired nerve are considered to become atrophic as already described.<sup>[8]</sup>

In cases with Mobius syndrome, marked hypoplasia of all EOMs was most prominent in their posterior aspects as has been demonstrated in the previous literature.<sup>[6,11,12]</sup>

We found splitting of lateral rectus in one case of bilateral congenital sixth nerve palsy, but not in any case of DRS though the previous study<sup>[6]</sup> has shown splitting in 2/5 (40%) of patients with Duane syndrome, considered secondary to dysgenesis of abducens nerve. Our finding suggest that congenital sixth nerve palsy may be a spectrum of DRS and the clinical picture differs due to the development of secondary dysinnervation in DRS.

Our study helps in understanding the pathogenesis of CCDDs as the primary pathology is the same in all cases where nerves are affected somewhere along their course (most

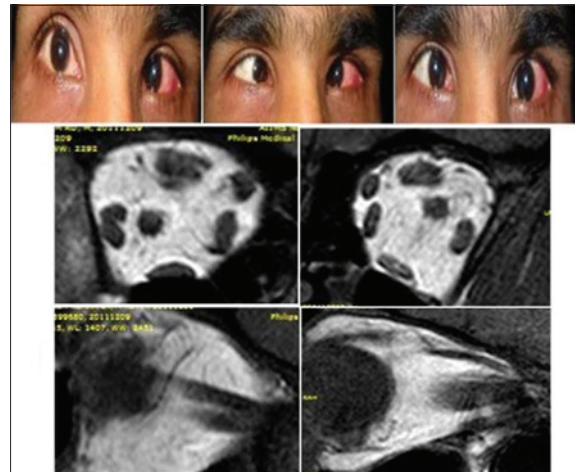


**Figure 3:** Clinical picture of Case 9 showing esodeviation in both eyes in primary gaze, and limitation of abduction in both eyes. Magnetic resonance imaging showing right eye lateral rectus splitting, in both coronal section and sagittal section (left) seen in comparison to normal lateral rectus in control in coronal and sagittal section (right)

**Table 5: Lateral rectus (diameter, area, and circumference) mean values in affected and unaffected eyes in comparison to controls**

	LRD (cm)	LRA (cm <sup>2</sup> )	LRC (cm)
Affected eyes (1)	0.8375±0.122	0.2358±0.0801	2.0775±0.317
Unaffected eyes (2)	1.0317±0.063	0.3183±0.037	2.47±0.126
Controls (3)	1.074±0.108	0.342±0.034	2.53±0.173
Comparison of 1 and 3	<i>P</i> <0.0001	<i>P</i> =0.01	<i>P</i> =0.001
Comparison of 2 and 3	<i>P</i> =1.0	<i>P</i> =1.0	<i>P</i> =1.0

LRD: Lateral rectus diameter, LRA: Lateral rectus area, LRC: Lateral rectus circumference

probable location is cranial nerve nucleus), and there is dysinnervation from adjacent nerves. More of such studies will help in knowing the complex variability of CCDDs. Additional research is needed to correlate these phenotypic changes with the underlying genotype changes. This should help to clearly understand why the various CCDDs are unique in themselves and may further lead us to correlate treatment plans not at just the phenotypic levels of strabismus surgery but also at the genetic level.

#### Financial support and sponsorship

Nil.

#### Conflicts of interest

There are no conflicts of interest.

#### References

- Gutowski NJ, Bosley TM, Engle EC. 110<sup>th</sup> ENMC International Workshop: The congenital cranial dysinnervation disorders (CCDDs). Naarden, the Netherlands, 25-27 October, 2002. *Neuromuscul Disord* 2003;13:573-8.
- Assaf AA. Congenital innervation dysgenesis syndrome (CID)/congenital cranial dysinnervation disorders (CCDDs). *Eye (Lond)* 2011;25:1251-61.
- Demer JL, Miller JM. Orbital imaging in strabismus surgery. In: Rosenbaum AL, Santiago AP, editors. *Clinical Strabismus Management: Principles and Surgical Techniques*. Philadelphia, PA, USA: WB Saunders; 1999. p. 84-8.
- Fischbach F, Müller M, Bruhn H. Magnetic resonance imaging of the cranial nerves in the posterior fossa: A comparative study of t2-weighted spin-echo sequences at 1.5 and 3.0 tesla. *Acta Radiol* 2008;49:358-63.
- Jiao YH, Zhao KX, Wang ZC, Qian XH, Wu X, Man FY. Magnetic resonance imaging of the ocular motor nerves in normal volunteers. *Zhonghua Yan Ke Za Zhi* 2009;45:219-24.
- Yonghong J, Kanxing Z, Zhenchang W, Xiao W, Xuehan Q, Fengyuan M, *et al.* Detailed magnetic resonance imaging findings of the ocular motor nerves in Duane's retraction syndrome. *J Pediatr Ophthalmol Strabismus* 2009;46:278-85.
- Demer JL, Ortube MC, Engle EC, Thacker N. High-resolution magnetic resonance imaging demonstrates abnormalities of motor nerves and extraocular muscles in patients with neuropathic strabismus. *J AAPOS* 2006;10:135-42.
- Okanobu H, Kono R, Miyake K, Ohtsuki H. Splitting of the extraocular horizontal rectus muscle in congenital cranial dysinnervation disorders. *Am J Ophthalmol* 2009;147:550-6.e1.
- Agrawal S, Singh V, Parihar A, Katiyar V, Srivastava RM, Chahal V. Magnetic resonance imaging (MRI) in Duane retraction syndrome. *J Clin Ophthalmol Res* 2016;4:137-41.
- Kang NY, Demer JL. Comparison of orbital magnetic resonance imaging in Duane syndrome and abducens palsy. *Am J Ophthalmol* 2006;142:827-34.
- Dumars S, Andrews C, Chan WM, Engle EC, Demer JL. Magnetic resonance imaging of the endophenotype of a novel familial Möbius-like syndrome. *J AAPOS* 2008;12:381-9.
- Wu SQ, Man FY, Jiao YH, Xian JF, Wang YD, Wang ZC. Magnetic resonance imaging findings in sporadic Möbius syndrome. *Chin Med J (Engl)* 2013;126:2304-7.